Available online at www.sciencedirect.com
SCIENCE DIRECT®
Phytochemistry 66 (2005) 2092–2107
PHYTOCHEMISTRY
www.elsevier.com/locate/phytochem

# Reassessment of effects on lignification and vascular development in the *irx4 Arabidopsis* mutant ☆

Ann M. Patten, Claudia L. Cardenas, Fiona C. Cochrane, Dhrubojyoti D. Laskar, Diana L. Bedgar, Laurence B. Davin, Norman G. Lewis *

*Institute of Biological Chemistry, Washington State University, P.O. Box 646340, Pullman, WA 99164-6340, USA*

Received 28 October 2004; received in revised form 4 December 2004
Available online 3 February 2005

**Abstract**

The *Arabidopsis thaliana irregular xylem4* (*irx4*) cinnamoyl-CoA reductase 1 (CCR1) mutant was reassessed for its purported exclusive rate-limiting or key effects on lignification. Analyses of gross growth characteristics and stem cross-section anatomy, from seedling emergence to senescence, revealed that stunted *irx4* mutant lines were developmentally delayed, which in turn *indirectly but predictably* led to modest reductions (ca. 10–15%) in overall lignin amounts. Such developmental changes are not generally observed in suppression of other monolignol pathway forming enzymes (e.g., 4-coumarate CoA ligase) even when accompanied by significant reductions in lignin amounts. With the greatly arrested development of the *irx4* mutant, formation of the lignin-derived syringyl moieties was also predictably delayed (by about 1–2 weeks), although at maturation the final guaiacyl:syringyl ratios were essentially identical to wild-type. No evidence was obtained for so-called abnormal lignin precursors being incorporated into the lignin, as shown by solid-state $^{13}C$ NMR spectroscopic analysis in contrast to a claim to the contrary [Jones, L., Ennos, A.R., Turner, S.R., 2001. Cloning and characterization of *irregular xylem4* (*irx4*): a severely lignin-deficient mutant of *Arabidopsis*. Plant J. 26, 205–216]. A previous claim of an ''abnormal'' lignin present in stunted CCR downregulated tobacco was also not substantiated, with only trace differences being noted in the presumed cell-wall constituent levels. More importantly, a linear correlation between total lignin amounts and lignin-derived fragmentation products was observed at all stages of *Arabidopsis* growth/development in both wild-type and *irx4* mutant lines, regardless of lignin content, i.e., in harmony with an exquisitely controlled and predictable macromolecular assembly process.

Recombinant CCR1 displayed fairly broad substrate versatility for all phenylpropanoid CoA substrates, with both feruloyl and 5-hydroxyferuloyl CoA being the best substrates. Taken together, these data indicate that other CCR isoforms are apparently capable of generating monolignol-derived lignified elements in *irx4* when CCR1 is impaired, i.e., indicative of a functionally redundant CCR metabolic network operative in *Arabidopsis*. Other dwarfed phenotypes have also been observed following downregulation/disruption of unrelated metabolic processes but which also involve CoA ester metabolism, i.e., with hydroxymethylglutaryl CoA reductases in *Arabidopsis* and a bacterial enoyl CoA hydratase/lyase overexpressed in tobacco. Although the reasons for dwarfing in each case are unknown, a common mechanism for the various pleiotropic effects is proposed through perturbation of CoASH pool levels. Finally, this study demonstrates the need for progressive analyses over the lifespan of an organism, rather than at a single time point which cannot reveal the progressive developmental changes occurring.


*Keywords:* *Arabidopsis thaliana*; Cruciferae; *irx4* mutant; Cinnamoyl-CoA reductase; Lignin; Growth and development; Histochemistry; Lignin analysis; Solid-state $^{13}C$ NMR spectroscopy; CoASH metabolism

☆ Data deposition: the sequence reported in this paper has been deposited in the GenBank database (accession number AY743921).

* Corresponding author. Tel.: +1 509 335 2682; fax: +1 509 335 8206.
*E-mail address:* lewisn@wsu.edu (N.G. Lewis).

0031-9422/$ - see front matter © 2005 Elsevier Ltd. All rights reserved.
doi:10.1016/j.phytochem.2004.12.016

## 1. Introduction

In order to begin to systematically define the precise physiological roles of various members of the annotated cinnamoyl-CoA reductase (CCR) multigene family (Costa et al., 2003), the *Arabidopsis thaliana irregular xylem4* (*irx4*) mutant of CCR1 (Jones et al., 2001) was comprehensively re-examined at various stages of plant growth and development through full maturation and senescence. This was to determine if its phenotype actually resulted from a specific regulatory (key) role in monolignol/lignin biosynthesis as claimed earlier (Jones et al., 2001), or was instead more likely a consequence of systemic perturbation of, for example, CoASH metabolism. In this context, physiological clarification of the roles of putative phenylpropanoid pathway genes (many of which, such as CCR, exist as multigene families) are being pursued in this laboratory as part of a National Science Foundation *Arabidopsis* 2010 project (Costa et al., 2003; Cochrane et al., 2004; Kim et al., 2004).

In silico analysis of the *Arabidopsis* genome sequence databases (Costa et al., 2003) indicated that there were some 11 annotated CCR homologues, of which only two isoforms had a previously designated function (CCR1 and CCR2). CCR1 is reportedly specific to monolignol biosynthesis/lignification (Lauvergeat et al., 2001), while mRNA transcripts from CCR2 (85.8% similarity and 82.8% identity to CCR1, Costa et al., 2003) were expressed in response to pathogen infection, i.e., suggesting but not proving a role in plant defense (Lauvergeat et al., 2001). Of the nine remaining putative CCR homologues, only two have been partially examined (Østergaard et al., 2001); the rest have not been functionally characterized in vitro or in vivo at any level. It is conceivable that some of these might also be part of a functionally redundant CCR metabolic network leading to the monolignols in specific cell types (Costa et al., 2003), as recently demonstrated for the cinnamyl alcohol dehydrogenase (CAD) gene family in *Arabidopsis* (Kim et al., 2004).

Curiously, CCR has been claimed to be a *key* regulatory enzyme of the monolignol-specific biosynthetic pathway, thereby controlling the quantity of lignin deposited (Piquemal et al., 1998; Jones et al., 2001; Goujon et al., 2003). Of course, any biochemical step in a pathway could become rate-limiting if it was sufficiently suppressed, but this does not by itself establish it to be a "normal" rate-limiting or regulatory process. On the other hand, metabolic flux and transcriptional profiling of the monolignol pathway gave no evidence that CCR *normally* has a rate-limiting or regulatory role (Anterola et al., 2002; Anterola and Lewis, 2002). In contrast, under "normal" metabolic flux conditions, carbon allocation to the pathway is determined by the availability of phenylalanine and the relative activities of cinnamate-4-hydroxylase and *p*-coumarate-3-hydroxylase, respectively. In fact, a recent study involving the down-regulation of both CCR and CAD obtained by crossing of individual anti-sense homozygous transgenic lines altered in CCR and CAD activities, actually implicated a synergistic interaction between these enzymes rather than a dominant (rate-limiting) role by one or the other (Chabannes et al., 2001). Thus, it seemed incongruous that the CCR1-*irx4 Arabidopsis* mutant would have a key rate-limiting/regulatory role in lignification, even though the researchers had reported a 50% reduction in overall lignin content in the dwarfed mutant (Jones et al., 2001); however, the appropriateness of direct comparison of wild-type (WT) and *irx4* phenotypes was questionable given that the *irx4* phenotype was greatly stunted, with pendulant, dark green flowering stems (having collapsed xylem cells attributed to lignin downregulation). Conclusions were also drawn from a very narrow scope of sampling with reliance on data from a single time point, thus affording no insight into developmental trends.

In this study, we comprehensively reassessed the putative CCR1-*irx4 Arabidopsis* mutant including evaluation of its stem tissue growth pattern and lignification response at all developmental stages until maturation. Such detailed temporal analyses were necessary in order to more fully assess phenotype, including characters not consistent over the lifespan of the plant (Boyes et al., 2001). Contrary to previous reports, it was established that only a very modest reduction in lignification in the *irx4* mutant actually occurred, relative to wild-type, this being a *secondary* effect of delayed growth and development. Other developmental alterations (e.g., in trichome formation), with no established relationship to lignification, were also observed suggesting that the chemically mutagenized *irx4* used in previous studies (Jones et al., 2001) had other mutations. However, the basis of these phenotypic differences was not investigated further.

Taken together, the available data thus provide further evidence that CCR1 does not have an exclusive rate-limiting role in monolignol biosynthesis/lignification. It is proposed instead that the phenotypes observed may be derived from perturbations in CoASH pool levels whose overall effect on metabolism leads to the various pleiotropic effects observed. Additionally, using solid-state $^{13}C$ NMR spectroscopy, no evidence was found for other non-monolignol moieties being incorporated into the lignin biopolymer as previously claimed, *albeit with no supporting data of any type* (Jones et al., 2001). In an analogous manner, claims that CCR down-regulation in tobacco (Ralph et al., 1998) resulted in incorporation of non-lignin monomers were also not substantiated (Anterola and Lewis, 2002). By contrast, in the present study, it was established that lignin deposition was both ordered and predictable at all developmental stages examined.

## 2. Results and discussion

The *Arabidopsis irx4* mutant (ecotype: Landsberg *erecta*, L*er*) was previously generated using ethyl methane sulphonate (EMS) and has reduced fertility and collapsed metaxylem elements (Jones et al., 2001) similar to the EMS-generated cellulose synthase mutants *irx1-3* and *5*; the latter were identified by sequence comparisons to those of bacterial cellulose synthase and those in the *Arabidopsis* genome, as well as by genetic complementation studies (Turner and Somerville, 1997; Taylor et al., 1999; Taylor et al., 2000; Taylor et al., 2003). Although the EMS treatment was considered to result in a single mutation in CCR1 in *irx4* (Jones et al., 2001), we observed that the mutant line segregated into two quite distinct populations (in a ca. 1 to 1 ratio), one with trichomes (i.e., as for WT) and one without, thereby suggesting the presence of more than one mutation (data not shown). The reasons for these differences were not pursued further, although this is the same mutant examined by Jones et al. (2001). Instead, it serves to underscore the importance of carefully monitoring phenotype differences.

The primary focus of the current study, however, was on the analysis and comparison of various characteristics of developing stem segments of the two *irx4* trichome phenotypes versus that of WT at different time intervals until maturation, with particular attention being placed on the vascular apparatus. Figs. 1(a) and (b) plot changes in overall stem length and basal stem width (during bolting and maturation) for the different lines. In all cases, *irx4* stem lengths and basal stem widths were significantly reduced relative to that of WT at maturation by ca. ~50% (Fig. 1(a)) and 40–50% (Fig. 1(b)), respectively. Furthermore, the overall growth of the *irx4* lines was stunted at all stages throughout their lifespans. Additionally, from a developmental perspective, both *irx4* phenotypes had smaller rosette sizes than that of wild type at 14 days, again indicative of a developmental delay as early as the vegetative state (data not shown). Such developmental delays could be anticipated to result in differences in cell wall maturation processes and, hence, in lignin deposition. Note that, by contrast, the Jones et al. (2001) study gave no description of either growth conditions, or the precise developmental stage(s) harvested for both WT and *irx4* mutant lines.

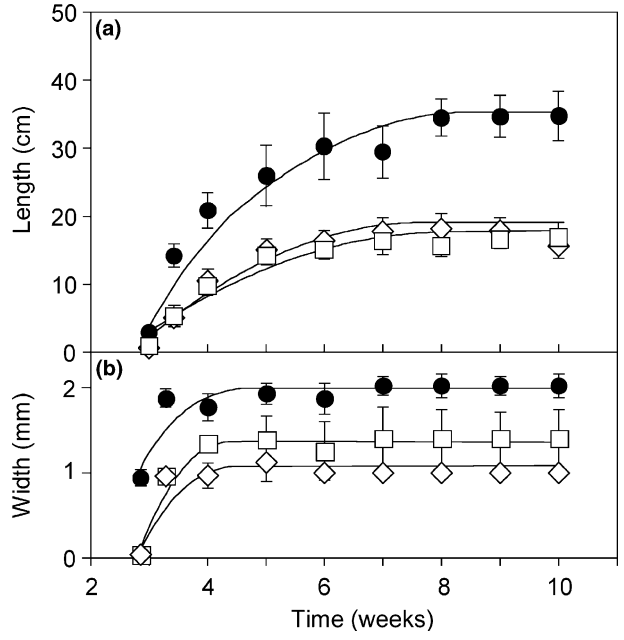


Fig. 1. Plot of changes in stem length (a) and basal stem width (b) of *Arabidopsis thaliana* (*Ler*) during growth and development until senescence. [All measurements are an average of 20 plants per sampling point.] ●, wild type (WT); ◇, *irx4* with trichomes and □, *irx4* without trichomes.

Developmental delay was also observed at the anatomical level using semi-thin stem sections from plants at 3.5 and 7 weeks of age, respectively (Fig. 2). Basal sections taken at 3.5 weeks, for example, clearly show that overall growth and development lags in *irx4* with comparatively smaller xylary and interfascicular regions (Fig. 2(b)) relative to WT (Fig. 2(a)), and have xylem (x) and interfascicular fiber (if) cell walls that visually appear either thinner and/or partially collapsed in the *irx4* lines (Fig. 2(b)), i.e., indicative (at least in part) of delayed cell differentiation. This trend is also evident earlier in development as observed in midstem sections taken at 3.5 weeks, where WT (Fig. 2(c)) shows comparatively more xylem (x) and xylary fiber precursor cells (see xf and arrowheads) and a more extensive zone of xylary cell differentiation (dx) relative to *irx4* (Fig. 2(d)). Effects of delayed development were also noted to persist in the *irx4* stem base at 7 weeks' growth and development, with the *irx4* stem diameter obviously greatly reduced (Fig. 2(f)) as are the xylem and interfascicular fiber (if) regions compared to WT (Fig. 2(e)). By early senescence (7 weeks), however, the *irx4* xylem and interfascicular fiber cells have apparently become fully lignified, albeit appearing to be compacted and even collapsed in the case of some metaxylem (mx) elements (Fig. 2(h)). By comparison, WT is of "normal" stem and cell size at this stage of early senescence (Fig. 2(g)). [These developmental delays in *irx4* were also observed at the middle and near the apex regions of stems at 3.5 and 7 weeks age (data not shown).]

It was next instructive to histologically detect lignin, in a qualitative manner, in the developing rachis (stem) of the *irx4* mutant and WT lines. Two protocols were used for lignin detection at the anatomical level; the phloroglucinol-HCl (Wiesner) reaction (Wiesner, 1878; Lewis and Yamamoto, 1990; Ruzin, 1999) was employed to detect putative coniferyl aldehyde end groups in guaiacyl (G) lignin (Adler et al., 1948; Adler and

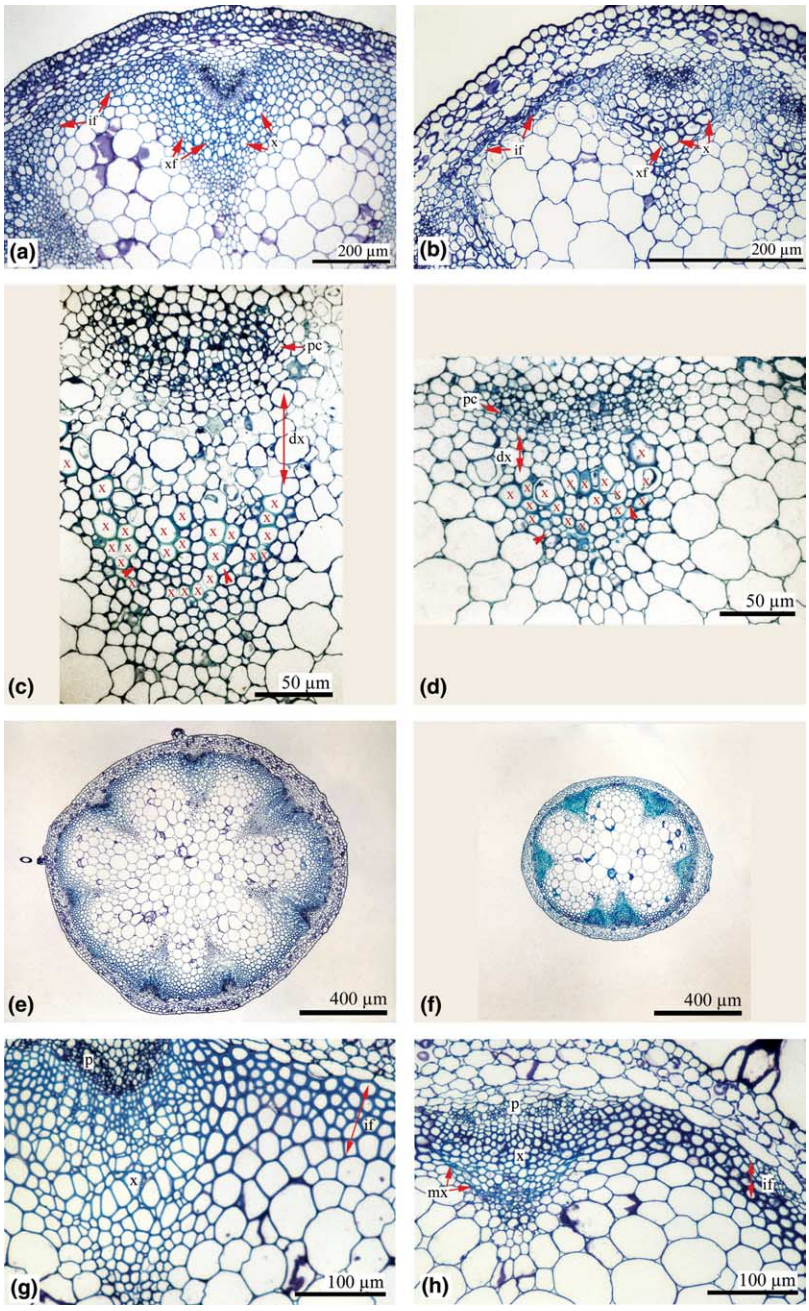


Fig. 2. Anatomy of *A. thaliana* (L*er*) wild type (WT) and *irx4* mutant stems at various stages of growth and development. (a–d) Cross-sections of 3.5-week-old *Arabidopsis* WT (a,c) and *irx4* mutant (b,d) taken at the base (a,b) or at midstem (c,d). (e–h) Stem cross-sections of 7-week-old *Arabidopsis* WT (e,g) and *irx4* mutant (f,h) taken at the base. Resin sections were stained with toluidine blue (a,b,e–f) or with Stevenel's Blue (c,d). dx, differentiating xylem; if, interfascicular fibers; mx, metaxylem, p, phloem; pc, procambium; x, xylem; xf and arrowheads, xylary fibers.

Ellmer, 1948; Sarkanen and Ludwig, 1971), whereas the Mäule reaction (Mäule, 1901) was used to visualize regions containing lignins with syringyl (S) moieties (Creighton et al., 1944; Towers and Gibbs, 1953; Sarkanen and Ludwig, 1971; Lewis and Yamamoto, 1990). The analyses of plant lines were carried out at 3.5, 5 and 7 weeks growth and development, this in turn reflecting early and late (maturation) stages of stem (rachis) growth. [While samples were analyzed near the apex, middle and base of stems at each developmental stage, only data are presented herein for the basal sections.]

For the WT line, G lignin deposition was clearly detectable in both xylem (x) and interfascicular fiber (if) regions of basal stem sections at 3.5 weeks (Fig. 3(a)), and subsequently throughout later developmental stages (5 and 7 weeks) until onset of senescence (Figs. 3(b) and (c)). In contrast, G lignin deposition in the *irx4* mutant was much delayed: at 3.5 weeks, faint phloroglucinol-HCl staining is only evident in early xylem

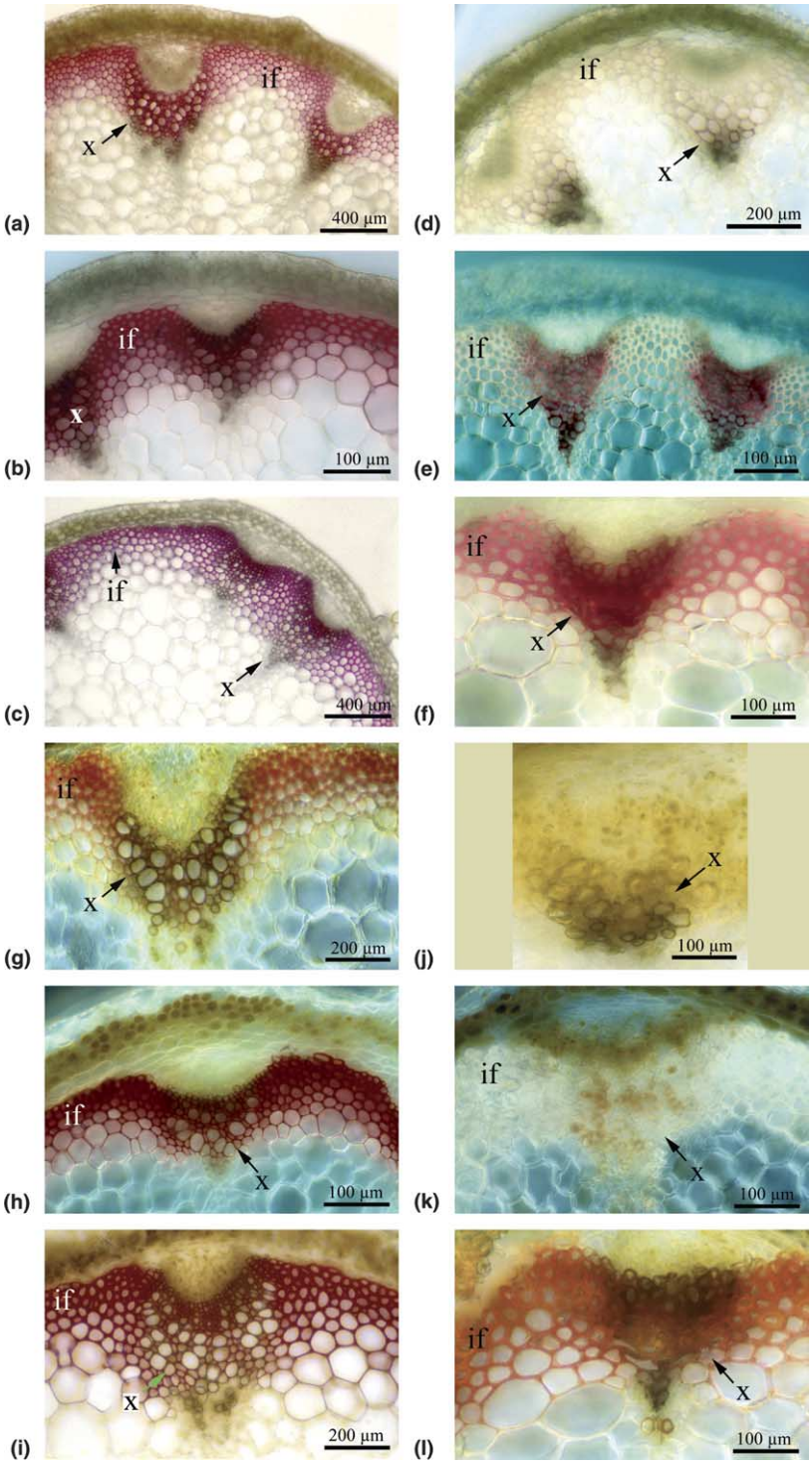


Fig. 3. Histochemical detection of anatomical regions containing guaiacyl and syringyl lignins in *A. thaliana* (L*er*) fresh basal stem sections of both wild type and *irx4* mutant lines at different stages of growth and development. (a–f) Sections were stained with phloroglucinol-HCl (Wiesner, 1878) at 3.5 (a,d), 5 (b,e) and 7 (c,f) weeks, respectively. (g–l) Sections were stained with the Mäule reagent (Mäule, 1901) at 3.5 (g,j), 5 (h,k) and 7 (i,l) weeks. Adjustments to magnification and illumination were made to allow optimal viewing of individual sections: Koehler optics were employed for a, c and i, whereas Nomarski optics were used in images b, d–h, and j–l, respectively. if, interfascicular region and x, xylem.

(Fig. 3(d)), but continues to ultimately encompass the xylem region by 5 weeks (Fig. 3(e)), and throughout the interfascicular fibers (if) by week seven (Fig. 3(f)). Likewise, qualitative S lignin deposition and localization were detected using the Mäule reagent: for WT, staining is evident in the fiber cells of the xylem region, and also into the interfascicular fibers (if) by 3.5 weeks (Fig. 3(g)), with this staining level increasing in intensity and

uniformity by weeks five and seven, i.e., until onset of senescence (Figs. 3(h) and (i)). In contrast, for the *irx4* mutant, there is essentially no S lignin detectable at 3.5 and 5 weeks (Figs. 3(j) and (k)), whereas at 7 weeks (maturation), it can be detected in xylem and interfascicular fiber (if) regions (Fig. 3(l)). This is consistent with the observed developmental delays.

Lignin contents and monomeric compositions were next estimated using both WT and *irx4* mutants from 3.5 to 10 weeks of growth and development through senescence. Protocols employed were the acetyl bromide (AcBr) method for estimating total lignin amounts (Iiyama and Wallis, 1990; Blee et al., 2001) and nitrobenzene oxidation (Iiyama and Lam, 1990; Blee et al., 2001)/thioacidolysis (Lapierre et al., 1986; Blee et al., 2001) methodologies to estimate monomeric compositions: the advantages and limitations of these approaches have been comprehensively described elsewhere (Anterola and Lewis, 2002).

AcBr lignin determinations were carried out at weekly intervals, as a function of stem growth and development, until plant senescence. From the data obtained (Fig. 4), the two CCR-*irx4* phenotypes had similar lignin contents (reported herein as % extractive-free cell wall residue, CWR) at all growth/developmental stages, with overall total amounts only reduced by approximately 10–15% at maturation/senescence when compared to WT. Interestingly, lignin deposition in the WT line reached maximum levels after about 7 weeks growth, this essentially mirroring trends noted previously for stem length growth (Fig. 1(a)). For the two *irx4* mutant lines, onset of lignification (relative to WT) was delayed by approximately 1–2 weeks, reaching maximum values at ca. 8–9 weeks. These data are thus in general agreement with the reduced number of (pre-lignified) xylem-forming cells observed in the dwarfed *irx4*

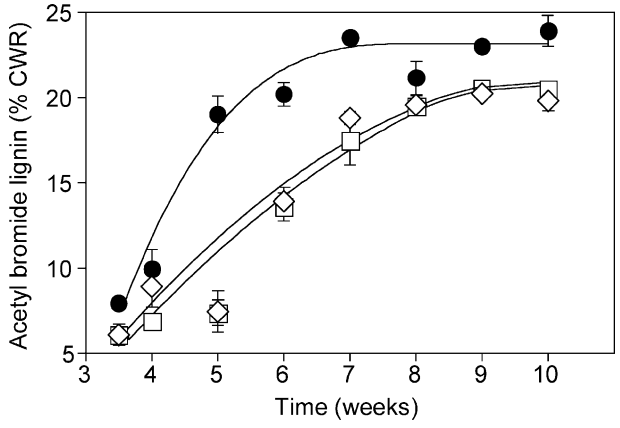


Fig. 4. Plot of acetyl bromide lignin determinations in stems at various stages of *A. thaliana* (L*er*) growth and development. ●, WT; ◇, *irx4* with trichomes and □, *irx4* without trichomes; CWR, cell wall residue of extractive-free plant stems.

phenotypes at various stages of development described earlier. These results thus indicate that the lignin contents in *irx4* are not reduced by ~50% as originally claimed (Jones et al., 2001), and that only modest changes in lignin levels actually occur at maturation; the latter is certainly not unexpected given the profound effects on growth and development observed for the *irx4* line(s) which in turn could be expected to give "reductions" in lignin amounts given that growth/development was adversely affected. These data thus underscore the necessity for systematic plant analyses at *all* stages of growth and development, rather than at one arbitrarily chosen time point, in order to identify the *meaningful* trends that actually occur. They also underscore the limitations in comparing *Arabidopsis* WT and dwarf mutants at different growth/developmental stages, even if the plants are of the same age.

Estimations of monomeric *p*-hydroxybenzaldehyde **1** (H), vanillin **2** (G) and syringaldehyde **3** (S) amounts released during alkaline nitrobenzene oxidation of the various extractive-free stem tissues were also carried out (Figs. 5(a)–(d)). It should be noted, however, that this method at best accounts for ca. 10–30% of the lignin present, and various types of phenylpropanoid moieties (e.g., cell-wall-bound hydroxycinnamic acids) can also release the corresponding H, G and S-derived aldehydes as summarized in Anterola and Lewis (2002). In spite of these limitations, release of the G, S and H components (Figs. 5(a)–(c)) at various stages of growth and development showed a near identical trend to that of the patterns of lignin deposition (Fig. 4), although the total recovered amounts of G, S and H constituents were ca. 20% lower than that of WT (Fig. 5(c)), in accordance with the slightly lower lignin contents of the *irx4* dwarfed mutant at maturation. Additionally, formation of the G component in the *irx4* phenotypes initially lagged slightly behind that of WT, prior to reaching maximum values by about 8 weeks (Fig. 5(a)). The S moieties, on the other hand, were only detectable at about 6 weeks development, reaching maximum levels at ca. 7–8 weeks (Fig. 5(b)); in all cases, only traces of the H-units could be detected (data not shown). Finally, the S/G ratios of the *irx4* lines were also initially lower at early stages of growth/development when compared to WT, but at maturation were essentially identical (Fig. 5(d)). These data, i.e., as regards to patterns of G and S lignin component deposition, thus showed similar trends to that observed for the lignin histological data (Fig. 3).

In a similar manner, thioacidolysis was used to estimate G/S monomeric compositions at various stages of growth and development (Figs. 5(e)–(h)). In contrast to alkaline nitrobenzene oxidation, this method is thought to only cleave 8-*O*-aryl linkages in the lignin biopolymers, with conversion of the cleaved G and S moieties into their 7,8,9-trithio derivatives **4**–**6**. The yields of thioacidolysis products as a percentage of

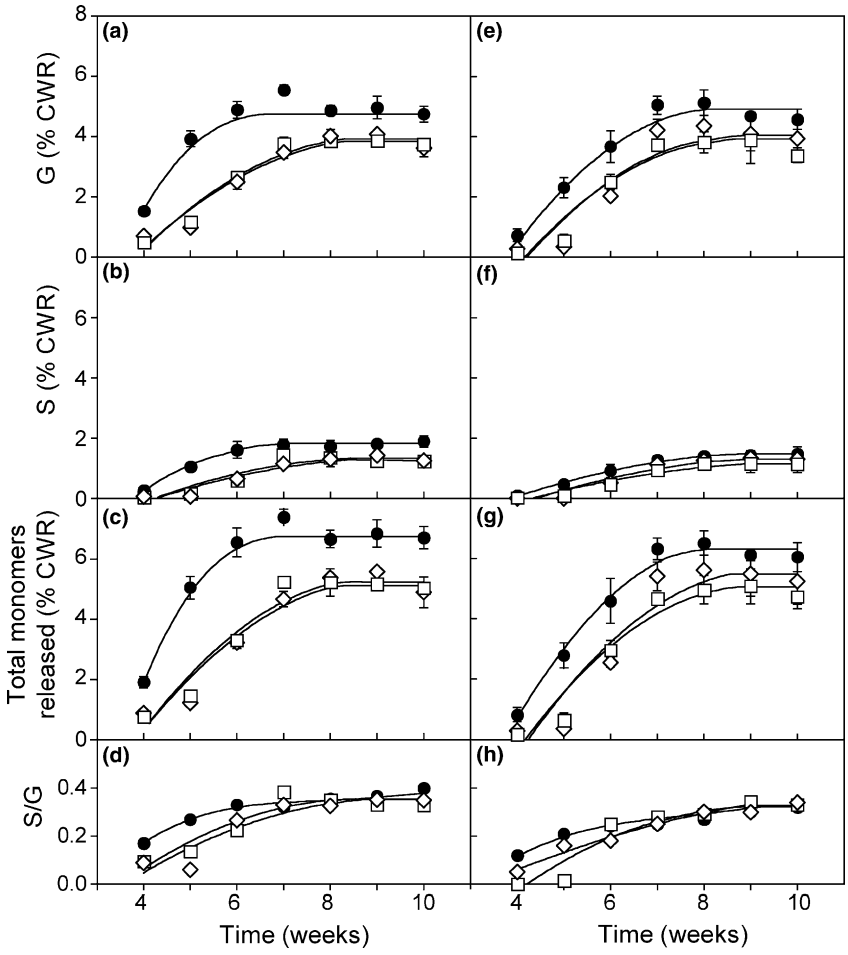


Fig. 5. Guaiacyl and syringyl contents in wild type *Arabidopsis* (L*er*) and *irx4* mutants. (a–c) Estimations of monomer amounts released during alkaline nitrobenzene oxidation of wild type and *irx4* extractive-free stem tissues. (d) Syringyl:guaiacyl (S/G) ratios determined by nitrobenzene oxidation. (e–g) Estimations of monomer amounts released during thioacidolysis of wild type and *irx4* extractive-free stem tissues. (h) Syringyl:guaiacyl (S/G) ratios determined by thioacidolysis. ●, WT; ◇, *irx4* with trichomes and □, *irx4* without trichomes; CWR, cell wall residue of extractive-free plant stems.

lignin present typically range from 10% to 30% (Anterola and Lewis, 2002).

The amounts of G and S units released during thioacidolysis in the *irx4* mutants are lower than that of WT during all stages of growth and development, and again lag behind WT by 1–2 weeks (Figs. 5(e)–(g)). As for alkaline nitrobenzene oxidation, the S-units are essentially only detectable by 6 weeks growth and development, reaching maximum values at ca. 8 weeks (Fig. 5(f)), with the S and G levels again being reduced by ca. 15–20% (Fig. 5(g)). Moreover, as noted with the alkaline nitrobenzene oxidation data, the S/G thioacidolysis ratios were also lower at early stages of stem bolting but became essentially identical at maturation to that of WT (Fig. 5(h)). Significantly, the total amounts of nitrobenzene and thioacidolysis oxidation fragments **1**–**3** and **4**–**6** released were essentially identical suggesting a common origin for both in the lignified tissues.

It was also instructive to compare the estimated (AcBr) lignin contents versus that of yield of products released by both nitrobenzene oxidation and thioacidolysis for the WT and *irx4* mutant lines at all stages of growth and development examined (Figs. 6(a) and (b)). Two significant observations were made: firstly, beyond ~5% estimated AcBr lignin content, there is a striking linear relationship between the amount of nitrobenzene (HGS, Fig. 6(a)) and thioacidolysis (GS, Fig. 6(b)) moieties liberated when plotted against AcBr lignin contents, regardless of whether mutant or WT line. This linear relationship is *independent* of the S/G ratios measured in either plant lines, these varying from 0.06 to 0.4 (see Fig. 5). That is, regardless of S/G ratio, the *total* amounts of the released lignin-derived fragments can be directly correlated with total (AcBr) lignin contents in a linear fashion. A possible explanation is that the inter-unit linkage *pattern* undergoing cleavage and monomer release in the native lignin biopolymer(s) is the same, regardless of either the nature of the monolignol moiety attached or lignin content. This is a finding of potentially considerable significance, i.e., as regards to

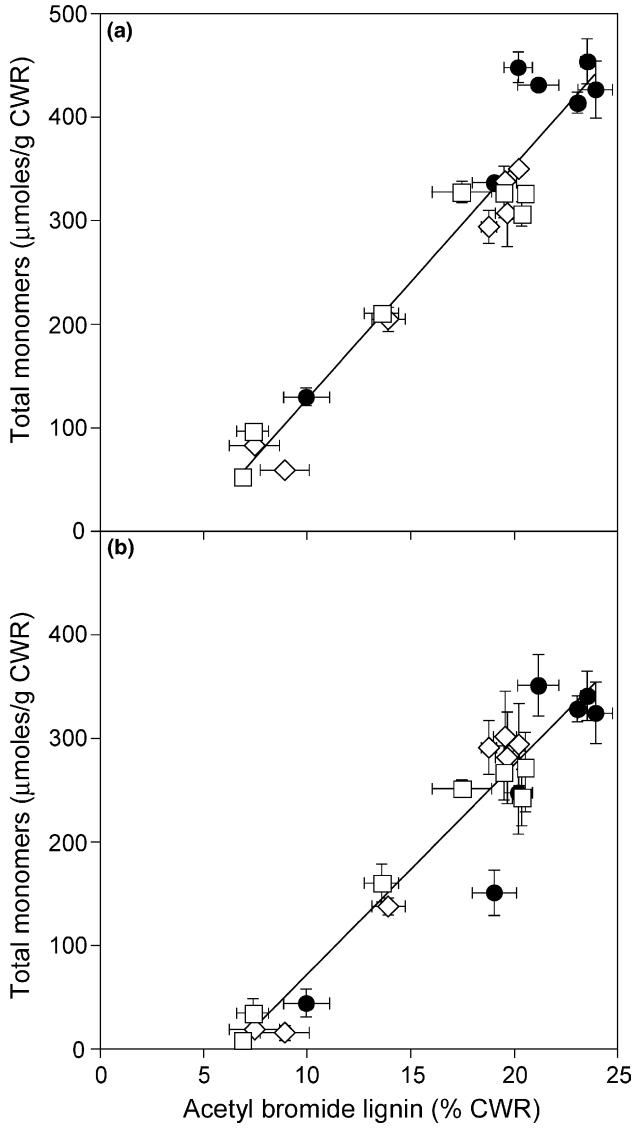


Fig. 6. Comparison of yields of presumed lignin-derived fragments released during either nitrobenzene oxidation or by thioacidolysis to that of total AcBr lignin contents. (a) Nitrobenzene oxidation. (b) Thioacidolysis. ●, WT; ◇, *irx4* with trichomes and □, *irx4* without trichomes; CWR, cell-wall residue of extractive-free plant stems.

predictable programmed/ordered native lignin macromolecular configuration and template polymerization (Guan et al., 1997; Sarkanen, 1998), and dirigent *site* (=radical binding site) guided formation of the native lignin primary chain (Davin and Lewis, 2000). Secondly, the plots of yields of presumed lignin-derived fragments versus total (AcBr) lignin amounts do not have a zero intercept (at the *X* and *Y* axes). This has been noted before (Anterola and Lewis, 2002) in *Arabidopsis* and other systems, and may be a consequence of either so-called "condensed" H-lignin deposition at the very earliest stages of lignin deposition (0–5%), thereby initially affording a biopolymer which essentially lacks cleavable 8-*O*-aryl bonds, or due to the presence of other UV-absorbing components (not necessarily lignin associated) that are laid down in earlier stages of vascular development. Determining the underlying reasons for this lack of zero intercept will be the subject of further inquiry.

Furthermore, in the previous study of Jones et al. (2001), it was repeatedly claimed that solid-state $^{13}C$ NMR spectroscopic analysis of the *irx4* mutant stem tissue, relative to wild type, revealed the presence of "abnormal" lignin monomers and "abnormal" lignin. However, no data of any kind was reported in support of this contention including what precise developmental stages were actually examined. It was therefore instructive to compare the solid-state $^{13}C$ NMR spectra of both the WT (Fig. 7(a)) and *irx4* mutant (Fig. 7(b)) stem tissue at maturation (9 weeks). Both spectra were essentially identical and gave no evidence for incorporation of non-lignin monomers within the lignin proper. In both spectra, the major resonances at ~74 and 72 ppm correspond to C-2, C-3 and C-5 of cellulose, whereas other signals at ~105, 89 (with a shoulder at 83) and ~64 ppm correspond to C-1, C-4 and C-6 (Lewis et al., 1987; Lewis et al., 1988; Eberhardt et al., 1993). Non-cellulosic aliphatic signals were also evident at ~56 ppm ($OCH_3$), with aliphatic methylenic resonances from 35 to 15 ppm. At lower field (>110 ppm), the resonance patterns were again very similar being mainly due to aliphatic, olefinic and carboxylic functionalities. Thus, there was no evidence to support the notion that "abnormal" lignin had been formed on the basis of either solid-state $^{13}C$ NMR spectroscopic analyses or chemical degradation. By contrast, the spectra were remarkably similar when taking into account the profound differences noted during growth/development.

Taken together the histochemical and lignin analysis data all indicate that during growth and development of the *irx4* mutant and WT lines, there are only very modest reductions in lignin contents with essentially identical S/G ratios at maturation, i.e., this being a consequence of arrested development. Comparable reductions in lignin levels have also been noted before for *Arabidopsis* (e.g., 4-coumarate-CoA ligase) (Lee et al., 1997; Anterola and Lewis, 2002) but these did *not* have the profound developmental changes as observed in this study, i.e. suggesting in the case of *irx4* that the effects on lignification are secondary. These data thus underscore: (1) the necessity to systematically study trends at all phases of growth and development and (2) that CCR-downregulated plants do not compensate for reduced lignin levels by utilizing other non-lignin compounds as claimed earlier (Ralph et al., 1997; Boudet, 1998; Ralph et al., 1998; Jones et al., 2001). The limitations of these latter claims have been addressed elsewhere (Anterola and Lewis, 2002), and need not be repeated other than to emphasize that claims of CCR downregulation in tobacco being accompanied by

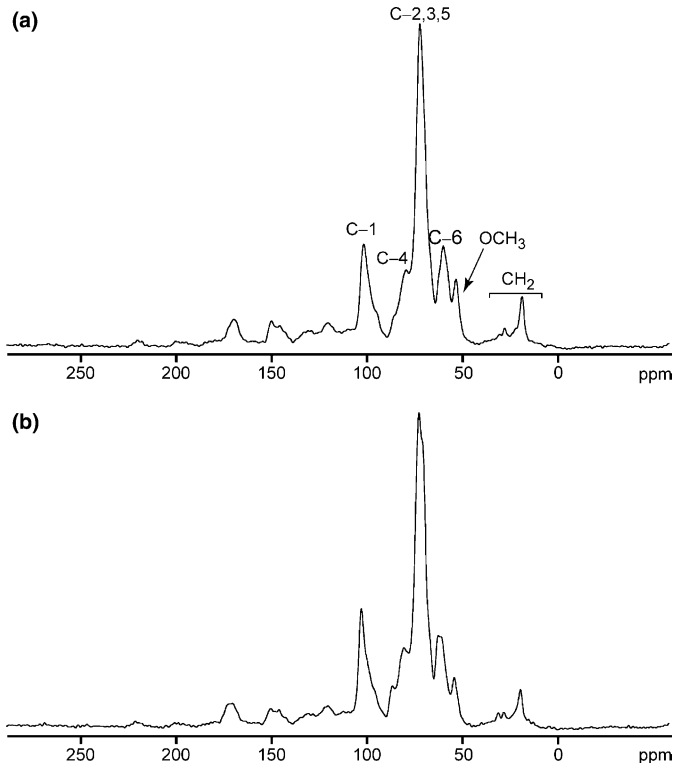


Fig. 7. Solid-state $^{13}C$ NMR spectra of (a) wild type *Arabidopsis thaliana* (L*er*) and (b) *irx4* mutant stem tissue at nine weeks growth (see Section 4 for sample preparation and NMR analysis conditions.)

significant increases in the levels of various hydroxyphenyl aldehydes and acids in the lignin (Chabannes et al., 2001) were not verifiable. The total amounts of these substances in the tobacco transgenic tissue barely differed between WT and CCR downregulated tobacco lines, i.e., only ranging from 0.04% to 0.06% of the cell-wall residue (Anterola and Lewis, 2002). Such differences represent only trace quantities and are presumably not significant.

Next, given that the H, G and S moieties in the lignin biopolymers were being formed in all cases, it was next instructive to ascertain if the CCR1 gene encoded a protein showing a marked preference for any of the potential substrates [i.e., *p*-coumaroyl (**7**), caffeoyl (**8**), feruloyl (**9**), 5-hydroxyferuloyl (**10**) and sinapoyl (**11**) CoA], or whether (as for the CAD multigene family, Kim et al., 2004), the enzyme displays broad substrate versatility for each. Earlier work (Lauvergeat et al., 2001) had suggested the latter to be the case, although only a limited number of the potential substrates [i.e., caffeoyl (**8**), feruloyl (**9**) and sinapoyl (**11**) CoA] were reported. Another factor suggesting substrate versatility of the various CCR isoforms was that the S/G ratios of the *irx4* mutants were the same as that of WT at maturation, even though *CCR1* had reportedly been disrupted. This presumably revealed that other members of the putative CCR multigene family effectively acted on the various substrates at some point(s) during growth/development, even if they were not temporally co-expressed. This may also explain why Jones et al. (2001) noted that "measurements of CCR activity proved inconclusive in the mutant" in their study.

The gene encoding AtCCR1 was thus next obtained by RT-PCR, with the corresponding recombinant functional protein expressed both in its native form as well as the C-terminal His-tagged analog. Both were purified to apparent homogeneity (Fig. 8) by various chromatographic steps; however, the kinetic properties of the two forms were found to differ substantially. Both native and His-tagged enzymes used *p*-coumaroyl (**7**), caffeoyl (**8**), feruloyl (**9**), 5-hydroxyferuloyl (**10**) and sinapoyl (**11**) CoA as substrates, but only the native CCR1 was active with cinnamoyl CoA (data not shown). The addition of the C-terminal His tag to CCR1 led to the enzyme exhibiting $K_m$ values significantly higher than that of the native CCR1; for instance, with feruloyl CoA (**9**), the $K_m$ was $110.5 \pm 11.8$ μM (His-CCR1) whereas for native CCR1 the $K_m$ was $3.0 \pm 0.8$ μM. The $V_{max}$ was also lower, thereby severely reducing overall enzyme efficiency ($k_{cat}/K_m$ 1470 $s^{-1}$ $M^{-1}$ His-CCR1 versus 518,890 $s^{-1}$ $M^{-1}$ for native CCR1, i.e., the native CCR was catalytically more efficient by a factor of ca. 350-fold higher). Reduction in enzyme efficiency was also apparently observed with the N-terminal

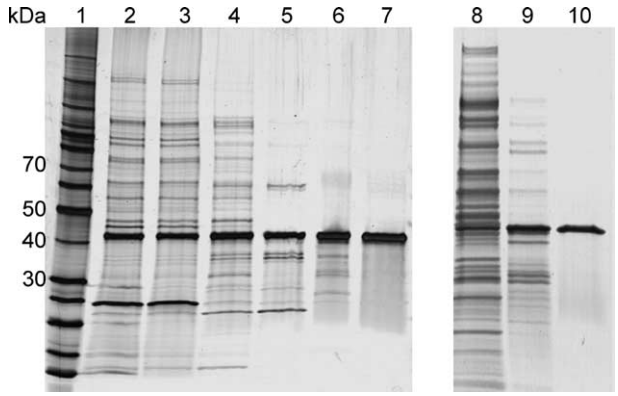


Fig. 8. SDS–PAGE showing the purification of CCR1. Native CCR1 Purification. Protein standards (Lane 1), crude cell lysate (Lane 2), ammonium sulphate/PD-10 (Lane 3), Q-Sepharose/ultrafiltration (Lane 4), MonoQ/ultrafiltration (Lane 5), Hydroxyapatite I/ultrafiltration (Lane 6) and Hydroxyapatite II/concentration (Lane 7). His-tagged CCR1 Purification. Crude cell lysate (Lane 8), and purity level following immobilized metal affinity (Lane 9) and hydroxyapatite (Lane 10) column chromatography.

glutathione *S*-transferase-CCR1 fusion protein purified by Lauvergeat et al. (2001), since a $k_{cat}/K_m$ of 39,600 $s^{-1}$ $M^{-1}$ for feruloyl CoA (**9**) was reported.

Native CCR1 was found to have a temperature and pH optima of 28–32 °C and 6.3–6.5 using the five phenylpropanoid thioesters (**7**–**11**) as potential substrates (Table 1). Overall, although CCR1 displayed similar affinities ($K_m$'s) for the substrates examined, it was catalytically most efficient ($k_{cat}/K_m$) with feruloyl (**9**), 5-hydroxyferuloyl (**10**), and sinapoyl (**11**) CoA rather than *p*-coumaroyl (**7**) and caffeoyl (**8**) CoA, e.g. by ca. 30–70-fold higher for feruloyl CoA (**9**) relative to caffeoyl (**8**) and *p*-coumaroyl (**7**) CoA, respectively. Comparable trends in overall substrate versatility have been noted in other studies with other plant species (Wengenmayer et al., 1976; Lüderitz and Grisebach, 1981; Sarni et al., 1984; Goffner et al., 1994; Lauvergeat et al., 2001). Nevertheless, in this study, all substrates were quite efficiently converted into the corresponding aldehydes, and as expected there was broad substrate versatility. Interestingly, all substrates displayed Michaelis–Menten kinetics over the concentration ranges examined (2–40 μM), except for sinapoyl CoA (**11**) with substrate inhibition at >25 μM; substrate inhibition also occurred with feruloyl (**9**) and 5-hydroxyferuloyl CoA (**10**) at concentrations >40 μM.

Thus, with the mutated AtCCR1 apparently not being expressed in functional form in the *irx4* mutant (Jones et al., 2001), it can be considered that formation of syringyl/guaiacyl lignin at maturation of the *irx4* mutant results from participation of other member(s) of the putative CCR gene family in *Arabidopsis*. In this regard, additional work is currently underway to establish the patterns of expression of each different member of the putative CCR family and to identify those involved in overlapping CCR metabolite networks proper, as already demonstrated for the cinnamyl alcohol dehydrogenase family (Kim et al., 2004).

## 3. Concluding remarks

In summary, the levels of lignin reduction obtained at maturation in the dwarfed/stunted *irx4* mutants are very modest (ca. 10–20%) at best, rather than the >50% reported by Jones et al. (2001) during an early stage of arrested development. The latter data, obtained at a single time-point during growth and development, also utilized the unreliable thioglycolic acid lignin determination method, a protocol with severe limitations (Anterola and Lewis, 2002). More importantly, however, it is noteworthy that the AcBr lignin, alkaline nitrobenzene oxidation and thioacidolysis analyses, together with that of solid-state $^{13}C$ NMR spectroscopy, all established that lignin biopolymers proper were being formed. That is, no evidence was obtained in this study in support of the notion that *Arabidopsis* mutant lines had compensated for even modest reductions in lignin levels by incorporating non-lignin monomers into the lignin biopolymer at any stage of growth and development. Yet, Jones et al. (2001) claimed that the *irx4* mutant employed novel non-lignin monomers in a compensatory role to offset reductions in lignin amounts, for which, however, experimental proof was *entirely* lacking. Furthermore, most – if not all – claims of non-lignin monomers (Ralph et al., 1997; Boudet, 1998) acting as lignin monomer surrogates have now been unequivocally disproven (Anterola and Lewis, 2002); others will be re-examined as necessary on a case-by-case basis.

Table 1
Kinetic parameters for AtCCR1

| AtCCR1 | Substrate | $K_m$ (μM) | $V_{max}$ (pkat $\mu g^{-1}$) | $k_{cat}$ ($s^{-1}$) | $k_{cat}/K_m$ ($s^{-1}$ $M^{-1}$) | Temperature optima (°C) | pH optima |
|---|---|---|---|---|---|---|---|
| Native | *p*-Coumaroyl CoA (**7**) | 13.7 ± 1.3 | 2.6 ± 0.1 | 0.10 | 7170 | 30 | 6.35–6.5 |
| | Caffeoyl CoA (**8**) | 7.1 ± 1.0 | 3.4 ± 0.2 | 0.13 | 17,870 | 30–32 | 6.35–6.5 |
| | Feruloyl CoA (**9**)[a] | 3.0 ± 0.8 | 41.4 ± 2.5 | 1.55 | 518,890 | 30 | 6.4–6.5 |
| | 5-OH Feruloyl CoA (**10**)[a] | 2.9 ± 0.6 | 37.0 ± 2.0 | 1.39 | 485,770 | 30 | 6.3–6.4 |
| | Sinapoyl CoA (**11**)[a] | 11.9 ± 4.1 | 29.1 ± 4.6 | 1.10 | 91,470 | 28–30 | 6.5 |
| His-Tagged | Feruloyl CoA (**9**) | 110.5 ± 11.8 | 4.0 ± 0.2 | 0.16 | 1470 | 28 | 6.5–6.75 |

[a] AtCCR1 showed substrate inhibition with sinapoyl CoA (**11**) (>25 μM) and with feruloyl (**9**)/5-hydroxyferuloyl (**10**) CoA (>40 μM).

As previously emphasized (Davin and Lewis, 2000), there is no other example in biochemistry whereby configuration of the main chain of a natural biopolymer could result from insertion of abnormal [monomeric non-monolignol] precursors, and such claims have not been verified in *independent* investigations.

The *irx4* mutant analysis in this study instead points to an overall delay in plant growth/development, and in associated plant cell wall formation including that of the vascular apparatus. Indeed, this is what Jones et al. (2001) actually observed, rather than a "severely lignin-deficient mutant of *Arabidopsis*" as claimed. Their carbohydrate analyses data actually provided convincing evidence for a systemic reduction in overall cell wall formation, since cellulose contents in *irx4* (as for lignin) were also reduced by 10–20%, as were hemicellulose component levels. That is, all the major cell-wall biopolymeric components were reduced in amount, this being consistent with the previously discussed impaired growth and development, including that of the *overall* vascular apparatus.

It needs also to be emphasized that even quite large reductions (up to 50%) in lignin levels, (such as noted for cinnamate-4-hydroxylase (C4H), Sewalt et al., 1997; Blount et al., 2000; Blee et al., 2001) in tobacco, 4-coumarate CoA ligase in *Arabidopsis* (Lee et al., 1997) and peroxidase in tobacco (Blee et al., 2003) were *not* apparently accompanied by any readily visible changes in growth and development of the phenotype; this in turn again indirectly suggests that the *irx4* mutant(s) impacts more than that of lignin deposition.

Accordingly, it is tempting to speculate that the phenotypic changes noted (dwarfing, etc.) may result from perturbation of CoASH metabolism. Similar dwarfed dark green phenotypes (as noted for *irx4*) have also been observed in *Arabidopsis* when 3-hydroxy-3-methylglutaryl coenzyme A reductase 1 (HMG1) is impaired (Suzuki et al., 2004), or in tobacco when a bacterial enoyl CoA hydratase/lyase is introduced and which partially converts *p*-coumaroyl CoA (**7**) and feruloyl CoA (**9**) [but not sinapoyl CoA (**11**)] into 4-hydroxybenzaldehyde (**1**)/vanillin (**2**) and acetyl CoA (Mayer et al., 2001); interestingly, the latter transformation also apparently affects metabolic flux into compounds such as chlorogenic acid. Thus, from first principles, it can be considered that with the CCR1 mutation (Jones et al., 2001) (or its downregulated form, Goujon et al., 2003), the levels of the corresponding cinnamoyl CoA substrates continue to accumulate until much, if not all, available CoASH is depleted, i.e., if no other CCR isoform was as metabolically active and/or co-expressed at that point. [Alternatively, the cinnamoyl CoA components could be metabolized into other non-lignin metabolites or shunt pathways.]

A similar situation can be envisaged for HMG1 impairment, where levels of HMG CoA would also be expected to increase until all CoASH was depleted (Suzuki et al., 2004), this perhaps also accounting for its similar unusual phenotype. Additionally, introduction of the bacterial enoyl CoA hydratase/lyase may also result in an increased build-up of acetyl CoA and thus reduced CoASH levels (Mayer et al., 2001). It, therefore, seems an attractive possibility that the various mutated/transgenic *Arabidopsis* and tobacco phenotypes result from systemic perturbation of CoASH levels, which in turn overall affects formation of the cell-wall/vascular apparatus in some manner yet to be defined.

Lastly, formation of G/S lignin in the *irx4* mutant reveals that during overall growth/development, one or more of the other putative CCR homologues engender formation of the corresponding H, G and S monolignols and thus of lignin formation. This, in turn, provides a very different interpretation from the lignocentric view that "a defect in CCR have confirmed the key role of this enzyme in determining the lignin content of the secondary wall" (Jones et al., 2001). This is certainly not the case, and emphasizes the necessity to study – in detail – developing trends via comprehensive analyses, rather than analyses at single time points. Future work will next be directed towards delineating the mechanistic/biochemical basis resulting in the dwarfed phenotype(s) and the relationship (as proposed) to CoASH metabolism, as well as in how the proposed CCR metabolic network is organized.

## 4. Experimental

### 4.1. General experimental procedures

Solid-state $^{13}C$ NMR spectra of WT and *irx4* stem tissue were obtained at 100 MHz on a Bruker Avance 400 spectrometer, equipped with a Chemagnetics double resonance probe-7.5 mm pencil type rotor. For acquisition of carbon-13 cross-polarization (CP) magic angle spinning (MAS) spectra, with $^{1}H$ decoupling, a recycle delay (4.0 s) and a spinning speed (5 kHz) were used; 1024 average scans were acquired, with chemical shifts given in $\delta$ ppm.

Protein purification employed both a Pharmacia LKB FPLC system equipped with a Monitor UV-M unit (native purification) and a BioCAD (Perseptive Biosystems) for native CCR1 purification and immobilized metal affinity chromatography for purification of the His-tagged CCR1. An Amicon stirred cell (Cell Model No. 8050) was used for ultrafiltration. Reversed-phase HPLC analyses of substrates and products were carried out on an Alliance 2695 HPLC system (Waters, Milford, MA) using a Symmetry Shield™ $RP_{18}$ column (Waters, $150 \times 3.9$ mm inner diameter). Thioacidolysis and nitrobenzene oxidation analyses were obtained using a HP 6890 Series GC System equipped with a DB-5MS

(Agilent technology; 30 m × 0.25 mm; 0.26 μm film thickness) column; product identity was obtained by mass spectrometric analysis using a HP 5973 MS detector (EI mode 70 eV). Measurements for acetyl bromide lignin analyses were carried out on a Lambda 20 spectrophotometer (Perkin–Elmer).

### 4.2. General Arabidopsis growth parameters

*Arabidopsis thaliana irx4* seeds were obtained from the *Arabidopsis* Biological Resource Center (ABRC) at Ohio State University (Columbus, OH). Seeds for both wild type (L*er*) and the *irx4* mutant were cold-stratified at 4 °C for at least 3 days before being sown on commercial soil (Sunshine mix #1). Plants were then grown in Washington State University greenhouses with day (14 h)/night (10 h) temperatures of 25/18 °C and fertilized at each irrigation with 200 ppm nitrogen based liquid fertilizer. The light intensity was 500–800 mmol $m^{-2}$ $s^{-1}$.

The CCR-*irx4* mutant line segregated into two populations in a ca. 1 to 1 ratio, one with stem trichomes (as in wild type) and one without; these phenotypes were distinguishable 3 weeks after seeding. The two distinct *irx4* stem trichome-phenotypes were independently evaluated for stem growth, development and maturation (length, width), as well as for patterns of plant cell-wall formation (i.e., particularly the lignified elements of stem tissues). Stem lengths and basal stem widths were measured from early stem bolt to senescence on a weekly basis (3.5–10 weeks), with measurements based on a minimum of 20 randomly chosen plants.

### 4.3. Arabidopsis morphological development and lignin histochemical analyses

Cell-wall anatomy at different stages of growth and development was examined using resin-embedded stem tissue. Fresh tissues were sectioned by hand and fixed with 2% (v/v) paraformaldehyde and 1.25% (v/v) glutaraldehyde in 50 mM PIPES buffer (pH 7.2) for 30 min at 25 °C. Tissues were individually rinsed in the same buffer (3 × 10 min) followed by dehydration using a standard EtOH series (Ruzin, 1999), then gradually embedded in medium grade L.R. White resin (London Resin, Co.) and heat polymerized at 60 °C. Semi-thin sections (1 μm) were stained with Stevenel's Blue or toluidine blue for 30 s, rinsed, dried and mounted in immersion oil.

Lignin histochemistry of various tissues at different stages of growth and development was examined using both Wiesner (1878) and Mäule (1901) reagents. The Wiesner reagent (phloroglucinol-HCl) was employed ostensibly to detect coniferyl aldehyde end groups in fresh hand-cut stem tissues (Sarkanen and Ludwig, 1971; Lewis and Yamamoto, 1990) as described by Ruzin (1999), whereas the Mäule reagent was used to detect syringyl moieties in fresh hand-cut stem tissues (Creighton et al., 1944; Towers and Gibbs, 1953; Lewis and Yamamoto, 1990) as described by Chapple et al. (1992). All light micrographs were recorded using an Olympus BH-2 photomicroscope and Kodak 64T film.

### 4.4. Stem tissue preparation for estimation of lignin contents/lignin monomer composition and solid-state $^{13}C$ NMR spectroscopic analysis

Lignin monomeric compositions and quantities were estimated from whole stem tissues, at various stages of growth and development, using the acetyl bromide lignin content (Iiyama and Wallis, 1990; Blee et al., 2001), thioacidolysis (Lapierre et al., 1986; Blee et al., 2001) and nitrobenzene oxidation (Iiyama and Lam, 1990; Blee et al., 2001) degradative methods, with all determinations based on % extractive-free cell wall residue. For all sampling points, plants were individually harvested, fast-frozen to −80 °C and freeze-dried for 36 h. Stem samples were then individually ball-milled (Fritsch Planetary Micro Mill) to a fine powder and sequentially extracted using EtOH/toluene (1:1, v/v), EtOH and $H_2O$ for 12 h per solvent with stirring at room temperature, with samples individually dried in vacuo, further ball-milled for 20 min and stored with desiccant until needed. For solid-state $^{13}C$ NMR spectroscopic analyses, ~250 mg of 9-week-old pre-extracted tissue samples were utilized. Acetyl bromide lignin contents were measured according to the method of Iiyama and Wallis (1990) and Blee et al. (2001) using extractive-free powdered stem tissue (4–6 mg), with an absorptivity value of 20.09 $g^{-1}$ l $cm^{-1}$ for the solubilized lignin. Lignin monomeric compositional analyses, as estimated by nitrobenzene oxidation, was carried out using extractive-free tissue samples (25–30 mg) as described by Iiyama and Lam (1990), with products identified by comparison of retention times to those of authentic standards and by mass-spectroscopic analysis using an HP 5973 MS detector in the EI mode (70 eV) (Blee et al., 2001). Thioacidolysis was carried out using extractive-free tissue samples (~10 mg) according to Lapierre et al. (1986), with products identified by comparison of both retention times and mass spectral fragmentation patterns with those of authentic synthetic standards (Blee et al., 2001).

### 4.5. Cloning and expression of CCR1

*Arabidopsis* Columbia and Landsberg ecotypes CCR1 have identical gene sequences. Thus, *Arabidopsis* (ecotype: Columbia) seedlings were harvested 8 days after seed was sown and immediately frozen in liquid nitrogen until needed. Total RNA was isolated using the RNeasy® Plant Mini kit (Qiagen®), with 5 μg

RNA used with random hexamers for first-strand cDNA synthesis as per the manufacturer's instructions (SuperScript™ First-Strand Synthesis System for RT-PCR, Invitrogen™). Touch-down PCR using gene-specific primers was applied to generate the CCR1 homologue, with the PCR carried out in a total volume (25 μl) containing 0.2 mM dNTP, 1.7 μg cDNA, 10× Expand HiFidelity buffer with $MgCl_2$, 1.3 U Expand HiFidelity Polymerase (Roche) with 10 pmol of each primer: CCR1For (5′AATATGCCAGTCGACGTAGCCTCA) and CCR1Rev (5′AGACCCGATCTTAATGCCATTTTC). A single PCR product of ~1 kb was recovered by gel purification using QIAquick Gel Extraction kit (Qiagen®) and cloned into pETBlue™-1 vector (Novagen) as well as pCRT7/CT TOPO® expression vector (Invitrogen™). The constructs' sequence and orientation were confirmed using both sense and antisense strands as templates before the CCR1 constructs were chemically transformed into *Escherichia coli* Tuner (DE3) cells (Novagen).

For native CCR1 (pETBlue™-1 construct) a single colony was incubated in 5 ml Luria–Bertani (LB) broth supplemented with carbenicillin (0.1 mg $ml^{-1}$) and grown overnight at 37 °C. The following day the inoculum was added to 300 ml LB media containing carbenicillin (0.1 mg $ml^{-1}$) and grown at 37 °C until reaching an $OD_{600}$ between 0.5 and 0.8 at which time isopropyl thio-β-D-galactoside (IPTG) was added (final concentration 1 mM). The bacteria were grown for a further 12 h at 37 °C then harvested by centrifugation (3000*g*, 25 min) and stored frozen at −80 °C until required. With the His-tagged CCR1 (pCRT7/CT construct) a single colony was used to inoculate an overnight starter culture of 5 ml LB broth supplemented with carbenicillin as before. The next day, the starter culture was used to inoculate 500 ml LB media (with carbenicillin, 0.1 mg $ml^{-1}$). The culture was grown at 37 °C until reaching an $OD_{600}$ of 0.7–0.9, at which time CCR1 protein induction was initiated by the addition of 0.1 mM IPTG. Cells were then grown for 20 h at 20 °C before harvesting by centrifugation. Cells were immediately frozen and stored at −80 °C until purification.

### 4.6. Protein purification

#### 4.6.1. Native AtCCR1 purification

Bacteria from 2 l LB were resuspended in Bugbuster Protein Extraction Reagent (40 ml), 1000 U Benzonase® Nuclease and 100 kU rLysozyme (Novagen) and agitated at 4 °C. Cellular debris was removed by centrifugation at 15,000*g* for 40 min. Supernatant was then fractionated with $(NH_4)_2SO_4$, with the 30–70% fraction recovered by centrifugation (15,000*g*, 40 min). The pellet was resuspended in a minimal volume of 20 mM Tris–HCl, pH 8, 1 mM EDTA and 1 mm DTT (Buffer A) and passed twice through pre-packed PD-10 Sephadex™ G-25M columns (Amersham Biosciences; ambient temperature) to desalt. The desalted protein was loaded onto a Q Sepharose Fast Flow anion-exchange column (Pharmacia Biotech; 12 cm × 1.6 cm; 1 ml $min^{-1}$) pre-equilibrated with Buffer A. After washing the column with Buffer A (1.2 column volume, CV), protein was eluted with a step gradient of 0.3 M NaCl which was sufficient to elute the majority of CCR1. Fractions containing CCR1 were pooled, desalted and concentrated by ultrafiltration (Amicon stirred cell with 30,000 MWCO [YM30] membrane; 4 °C). The retentate was loaded onto a MonoQ anion exchange column (Pharmacia Biotech; 10 cm × 1 cm) equilibrated in Buffer A at a flow rate of 2 ml $min^{-1}$. After washing the column with Buffer A (2.5 CV), a linear gradient from 0 to 0.14 M NaCl (2.5 CV) was applied whereupon the concentration established was held for an additional 1.5 CV. Active fractions containing CCR were pooled, desalted and concentrated by ultrafiltration (as mentioned above) and the buffer exchanged to 5 mM sodium phosphate, pH 7.4, 1 mM DTT (Buffer B) before the protein was loaded onto a hydroxyapatite column (Bio-Gel® HTP Gel; BioRad; 7.5 cm × 1.5 cm), pre-equilibrated with Buffer B at a flow rate of 1 ml $min^{-1}$. Unbound proteins were removed first by washing with 60 mM sodium phosphate (1.3 CV), after which the majority of CCR1 was eluted with 100 mM sodium phosphate. The active fractions were pooled and concentrated by ultrafiltration prior to the retentate being reapplied to the hydroxyapatite column. The column was washed first with Buffer B (1 CV), then 50 mM sodium phosphate (1.5 CV). A linear gradient from 50 to 80 mM was next applied over 20 min (1.5 CV) during which CCR1 was eluted. Fractions containing only CCR1 were pooled, concentrated with Centricon concentrators (Amicon) and used directly in assays. Aliquots from each step were analyzed by SDS–polyacrylamide gel electrophoresis using Laemmli's buffer system under denaturing and reducing conditions (Laemmli, 1970). Protein was separated on a 4–15% SDS–PAGE gradient gel and visualized by either Coomassie Blue or silver staining (Amersham Bioscience Application Note).

#### 4.6.2. His-tagged AtCCR1 purification

The cell pellet (from 250 ml culture) was resuspended in Bugbuster Protein Extraction Reagent (10 ml), 250 U Benzonase® Nuclease and 30 kU rLysozyme, and agitated at 500 rpm on an orbital shaker for 10 min at ambient temperature. The suspension was centrifuged at 15,000*g* then filtered (0.45 μm syringe filter; Acrodisc®) before purification by immobilized metal affinity chromatography. A POROS 20 MC column (10 cm × 0.46 cm) was pre-equilibrated with Buffer A (20 mM Tris–HCl, pH 7.9, 500 mM NaCl, 5 mM imidazole) at a flow rate of 10 ml $min^{-1}$. Aliquots (1 ml) of CCR1 filtrate were loaded onto the column; unbound

proteins were removed first by washing the column with Buffer B (20 mM Tris–HCl, pH 7.9, 500 mM NaCl, 50 mM imidazole; 7 CV). CCR1 was eluted with 110–300 mM imidazole using a linear gradient from Buffer B to Buffer C (20 mM Tris–HCl, pH 7.9, 500 mM NaCl, 500 mM imidazole; 15 CV) with 1 ml fractions being collected. Aliquots (10 μl) of the fractions were analyzed by SDS–polyacrylamide gel electrophoresis using a 4–15% gradient gel and visualization by silver staining. Fractions containing CCR1 were pooled and concentrated using Centricon Plus-80 microfugal filters (Amicon), diluted with 20 mM Tris–HCl (pH 7.5) and reconcentrated. The protein was desalted using a pre-packed PD-10 column (ambient temperature) prior to addition to a 0.5 ml hydroxyapatite column pre-equilibrated with 5 mM sodium phosphate (pH 6.8). A step gradient of 75 (4 CV), 100 (3 CV), 120 (3 CV) and 150 mM (3 CV) sodium phosphate (pH 6.8) was applied to the column with 1.5 ml fractions collected. CCR1 was eluted with 100–150 mM sodium phosphate (pH 6.8), pooled, and used for assays.

### 4.7. Enzyme assays

#### 4.7.1. General assays

Initial enzyme assays were carried out to determine enzyme activity with five potential substrates: *p*-coumaroyl (**7**), caffeoyl (**8**), feruloyl (**9**), 5-hydroxyferuloyl (**10**) and sinapoyl (**11**) CoAs. The five thioester substrates were synthesized using recombinant At4CL1 and At4CL5 (see Costa et al., 2003 for At4CL annotation), based on the method of Beuerle and Pichersky (2002). Each assay consisted of 160 μM β-NADPH, 40 μM of the respective substrate, CCR1 and 100 mM potassium phosphate buffer (pH 6.5) in a 250 μl volume. All assays were preincubated for 2 min at 30 °C (in a temperature-controlled shaking waterbath) prior to initiation by substrate addition and stopped by acidification (10 μl glacial AcOH). Controls with either no substrate or no enzyme were also performed for each substrate. Assays were carried out in triplicate and assay products were separated by reversed-phase HPLC with a 100 mM ammonium acetate:12.5% AcOH (v/v; Solvent A) and $CH_3CN$ (Solvent B) gradient at a flow rate of 1 ml $min^{-1}$ and detection of the aldehydes at 340 nm. The column was pre-equilibrated in solvent A; after introduction of the sample, a concave gradient (Waters, curve 8) from 100% A to A:B (72:28) over 32 min was carried out, followed by a linear gradient from A:B (72:28) to A:B (25:75) in 3 min and finally a convex gradient (Waters, curve 5) A:B (25:75) to 100% A in 3 min, this being held for 12 min to re-equilibrate the column. Monitoring of the CoA esters was also carried out at the following wavelengths: *p*-coumaroyl CoA (**7**), 324 nm; feruloyl CoA (**9**), 340 nm; caffeoyl (**8**) and 5-hydroxyferuloyl (**10**) CoAs, 342 nm and sinapoyl CoA (**11**), 344 nm. Calibration curves were established for each of the cinnamyl aldehydes **12**–**16** prior to assays.

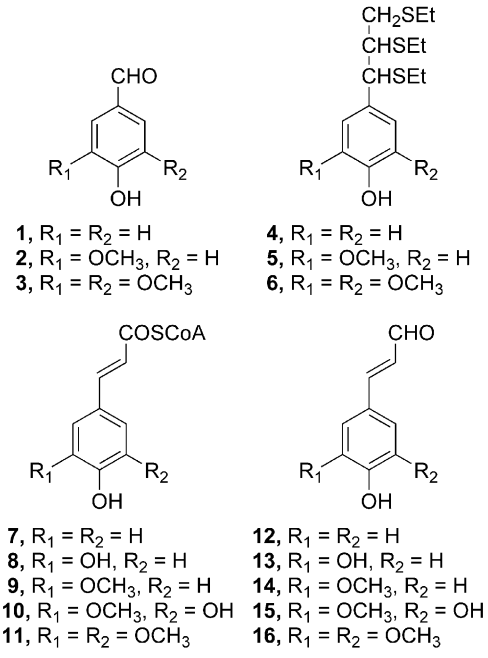


#### 4.7.2. Temperature and pH assays

CCR1 from the first hydroxyapatite purification stage (native purification) was used for both temperature and pH assays. For pH, a range of phosphate buffers (5.75–8) were tested at 30 °C. CCR1 (0.82 μg) was individually assayed with feruloyl (**9**) and sinapoyl (**11**) CoA for 1 min, with 5-hydroxyferuloyl CoA (**10**) for 2 min and with caffeoyl (**8**) and *p*-coumaroyl (**7**) CoA for 5 min. For temperature, a range from 14 to 55 °C was used with each substrate assayed at a constant pH of 6.5 (100 mM potassium phosphate) and with 0.68 μg CCR1. Assay times for each substrate were: 1 min for feruloyl (**9**) and sinapoyl (**11**) CoA, 2 min for 5-hydroxyferuloyl CoA (**10**), 4 min for caffeoyl CoA (**8**), and 5 min for *p*-coumaroyl CoA (**7**).

#### 4.7.3. Kinetic assays

For kinetic assays, a range of substrate concentrations from 2 to 80 μM was carried out. Each 250 μl assay contained 100 mM potassium phosphate (pH 6.4), 160 μM β-NADPH, purified CCR1 [0.24 μg for feruloyl CoA (**9**), 0.4 μg for sinapoyl (**11**) and 5-hydroxyferuloyl (**10**) CoA and 0.6 μg for caffeoyl CoA (**8**) and *p*-coumaroyl (**7**) CoA], and the thioester substrate. All assays were preincubated at 30 °C for 2 min in a temperature controlled waterbath prior to initiation by substrate addition. Assays were incubated for either 1 min [feruloyl,

sinapoyl and 5-hydroxyferuloyl CoA (**9**), (**11**) and (**10**)] or 5 min [caffeoyl and *p*-coumaroyl CoA (**8**) and (**7**)]. An aliquot (80 μl) of each assay mixture was then subjected to HPLC analysis as described above. $K_m$ and $V_{max}$ values were obtained from Michaelis–Menten plots, although with sinapoyl CoA (**11**) inhibition was noted at >25 μM and with feruloyl (**9**)/5-hydroxyferuloyl (**10**) CoA (>40 μM).

## Acknowledgments

This work was supported by the National Science Foundation *Arabidopsis* 2010 (MCB-0117260), the National Aeronautics and Space Administration (NAG 2-1513) and the G. Thomas and Anita Hargrove Center for Plant Genomic Research. The authors thank Derek Pouchnik and Gerhard Munske of the WSU Laboratory for Biotechnology and Bioanalysis for DNA sequencing, and Buhyun Youn for helpful advice on AtCCR1 purification. Thanks are also extended to Vincent R. Franceschi, Christine Davitt and Valerie Lynch-Holm of the WSU Electron Microscopy Center for advice regarding micrography, as well as to Dan Mitchell for acquisition of solid state $^{13}C$ NMR spectra.

## References

Adler, E., Björkqvist, K.J., Häggroth, S., 1948. Über die Ursache der Farbreaktionen des Holzes. Acta Chem. Scand. 2, 93–94.

Adler, E., Ellmer, L., 1948. Coniferylaldehydgruppen im Holz und in isolierten Ligninpräparaten. Acta Chem. Scand. 2, 839–840.

Anterola, A.M., Jeon, J.-H., Davin, L.B., Lewis, N.G., 2002. Transcriptional control of monolignol biosynthesis in *Pinus taeda*. Factors affecting monolignol ratios and carbon allocation in phenylpropanoid metabolism. J. Biol. Chem. 277, 18272–18280.

Anterola, A.M., Lewis, N.G., 2002. Trends in lignin modification: a comprehensive analysis of the effects of genetic manipulations/mutations on lignification and vascular integrity. Phytochemistry 61, 221–294.

Beuerle, T., Pichersky, E., 2002. Enzymatic synthesis and purification of aromatic coenzyme A esters. Anal. Biochem. 302, 305–312.

Blee, K., Choi, J.W., O'Connell, A.P., Jupe, S.C., Schuch, W., Lewis, N.G., Bolwell, G.P., 2001. Antisense and sense expression of cDNA coding for CYP73A15, a class II cinnamate-4-hydroxylase, leads to a delayed and reduced production of lignin in tobacco. Phytochemistry 57, 1159–1166.

Blee, K.A., Choi, J.W., O'Connell, A.P., Schuch, W., Lewis, N.G., Bolwell, G.P., 2003. A lignin-specific peroxidase in tobacco whose antisense suppression leads to vascular tissue modification. Phytochemistry 64, 163–176.

Blount, J.W., Korth, K.L., Masoud, S.A., Rasmussen, S., Lamb, C., Dixon, R.A., 2000. Altering expression of cinnamic acid 4-hydroxylase in transgenic plants provides evidence for a feedback loop at the entry point into the phenylpropanoid pathway. Plant Physiol. 122, 107–116.

Boudet, A.M., 1998. A new view of lignification. Trends Plant Sci. 3, 67–71.

Boyes, D.C., Zayed, A.M., Ascenzi, R., McCaskill, A.J., Hoffman, N.E., Davis, K.R., Görlach, J., 2001. Growth stage-based phenotypic analysis of *Arabidopsis*: a model for high throughput functional genomics in plants. Plant Cell 13, 1499–1510.

Chabannes, M., Barakate, A., Lapierre, C., Marita, J.M., Ralph, J., Pean, M., Danoun, S., Halpin, C., Grima-Pettenati, J., Boudet, A.M., 2001. Strong decrease in lignin content without significant alteration of plant development is induced by simultaneous down-regulation of cinnamoyl CoA reductase (CCR) and cinnamyl alcohol dehydrogenase (CAD) in tobacco plants. Plant J. 28, 257–270.

Chapple, C.C.S., Vogt, T., Ellis, B.E., Somerville, C.R., 1992. An *Arabidopsis* mutant defective in the general phenylpropanoid pathway. Plant Cell. 4, 1413–1424.

Cochrane, F.C., Davin, L.B., Lewis, N.G., 2004. The *Arabidopsis* phenylalanine ammonia-lyase multigene family: kinetic characterization of the four PAL isoforms. Phytochemistry 65, 1557–1564.

Costa, M.A., Collins, R.E., Anterola, A.M., Cochrane, F.C., Davin, L.B., Lewis, N.G., 2003. An *in silico* assessment of gene function and organization of the phenylpropanoid pathway metabolic networks in *Arabidopsis thaliana* and limitations thereof. Phytochemistry 64, 1097–1112.

Creighton, R.H.J., Gibbs, R.D., Hibbert, H., 1944. Studies on lignin and related compounds. LXXV. Alkaline nitrobenzene oxidation of plant materials and application to taxonomic classification. J. Am. Chem. Soc. 66, 32–37.

Davin, L.B., Lewis, N.G., 2000. Dirigent proteins and dirigent sites explain the mystery of specificity of radical precursor coupling in lignan and lignin biosynthesis. Plant Physiol. 123, 453–461.

Eberhardt, T.L., Bernards, M.A., He, L., Davin, L.B., Wooten, J.B., Lewis, N.G., 1993. Lignification in cell suspension cultures of *Pinus taeda*. *In situ* characterization of a gymnosperm lignin. J. Biol. Chem. 268, 21088–21096.

Goffner, D., Campbell, M.M., Campargue, C., Clastre, M., Borderies, G., Boudet, A., Boudet, A.M., 1994. Purification and characterization of cinnamoyl-coenzyme A:NADP oxidoreductase in *Eucalyptus gunnii*. Plant Physiol. 106, 625–632.

Goujon, T., Ferret, V., Mila, I., Pollet, B., Ruel, K., Burlat, V., Joseleau, J.-P., Barrière, Y., Lapierre, C., Jouanin, L., 2003. Down-regulation of the *AtCCR1* gene in *Arabidopsis thaliana* : effects on phenotype, lignins and cell wall degradability. Planta 217, 218–228.

Guan, S.-y., Mlynár, J., Sarkanen, S., 1997. Dehydrogenative polymerization of coniferyl alcohol on macromolecular lignin templates. Phytochemistry 45, 911–918.

Iiyama, K., Lam, T.B.T., 1990. Lignin in wheat internodes. Part 1: the reactivities of lignin units during alkaline nitrobenzene oxidation. J. Sci. Food Agric. 51, 481–491.

Iiyama, K., Wallis, A.F.A., 1990. Determination of lignin in herbaceous plants by an improved acetyl bromide procedure. J. Sci. Food Agric. 51, 145–161.

Jones, L., Ennos, A.R., Turner, S.R., 2001. Cloning and characterization of *irregular xylem4* (*irx4*): a severely lignin-deficient mutant of *Arabidopsis*. Plant J. 26, 205–216.

Kim, S.-J., Kim, M.-R., Bedgar, D.L., Moinuddin, S.G.A., Cardenas, C.L., Davin, L.B., Kang, C.-H., Lewis, N.G., 2004. Functional reclassification of the putative cinnamyl alcohol dehydrogenase multigene family in *Arabidopsis*. Proc. Natl. Acad. Sci. USA 101, 1455–1460.

Laemmli, U.K., 1970. Cleavage of structural proteins during the assembly of the head of bacteriophage T4. Nature 277, 680–685.

Lapierre, C., Monties, B., Rolando, C., 1986. Thioacidolysis of poplar lignins: identification of monomeric syringyl products and characterization of guaiacyl-syringyl lignin fractions. Holzforschung 40, 113–118.

Lauvergeat, V., Lacomme, C., Lacombe, E., Lasserre, E., Roby, D., Grima-Pettenati, J., 2001. Two cinnamoyl-CoA reductase (CCR) genes from *Arabidopsis thaliana* are differentially expressed during

development and in response to infection with pathogenic bacteria. Phytochemistry 57, 1187–1195.

Lee, D., Meyer, K., Chapple, C., Douglas, C.J., 1997. Antisense suppression of 4-coumarate: coenzyme A ligase activity in *Arabidopsis* leads to altered lignin subunit composition. Plant Cell 9, 1985–1998.

Lewis, N.G., Razal, R.A., Dhara, K.P., Yamamoto, E., Bokelman, G.H., Wooten, J.B., 1988. Incorporation of [2-$^{13}$C]ferulic acid, a lignin precursor, into *Leucaena leucocephala* and its analysis by solid state $^{13}$C NMR. J. Chem. Soc., Chem. Commun., 1626–1628.

Lewis, N.G., Yamamoto, E., 1990. Lignin: occurrence, biogenesis and biodegradation. Annu. Rev. Plant Phys. Plant Mol. Biol. 41, 455–496.

Lewis, N.G., Yamamoto, E., Wooten, J.B., Just, G., Ohashi, H., Towers, G.H.N., 1987. Monitoring biosynthesis of wheat cell wall phenylpropanoids *in situ*. Science 237, 1344–1346.

Lüderitz, T., Grisebach, H., 1981. Enzymic synthesis of lignin precursors. Comparison of cinnamoyl-CoA reductase and cinnamyl alcohol:NADP$^+$ dehydrogenase from spruce (*Picea abies* L.) and soybean (*Glycine max* L.). Eur. J. Biochem. 119, 115–124.

Mäule, C., 1901. Das Verhalten verholzter Membranen gegen Kaliumpermanganat, eine Holzreaktion neuer Art. Beiträge zur wissenschaftlichen Botanik 4, 166–185.

Mayer, M.J., Narbad, A., Parr, A.J., Parker, M.L., Walton, N.J., Mellon, F.A., Michael, A.J., 2001. Rerouting the plant phenylpropanoid pathway by expression of a novel bacterial enoyl-CoA hydratase/lyase enzyme function. Plant Cell 13, 1669–1682.

Østergaard, L., Lauvergeat, V., Næsted, H., Mattsson, O., Mundy, J., 2001. Two differentially regulated *Arabidopsis* genes define a new branch of the DFR superfamily. Plant Sci. 160, 463–472.

Piquemal, J., Lapierre, C., Myton, K., O'Connell, A., Schuch, W., Grima-Pettenati, J., Boudet, A.M., 1998. Down-regulation of cinnamoyl-CoA reductase induces significant changes of lignin profiles in transgenic tobacco plants. Plant J. 13, 71–83.

Ralph, J., Hatfield, R.D., Piquemal, J., Yahiaoui, N., Pean, M., Lapierre, C., Boudet, A.M., 1998. NMR characterization of altered lignins extracted from tobacco plants down-regulated for lignification enzymes cinnamyl-alcohol dehydrogenase and cinnamoyl-CoA reductase. Proc. Natl. Acad. Sci. USA 95, 12803–12808.

Ralph, J., MacKay, J.J., Hatfield, R.D., O'Malley, D.M., Whetten, R.W., Sederoff, R.R., 1997. Abnormal lignin in a loblolly pine mutant. Science 277, 235–239.

Ruzin, S.E., 1999. Plant Microtechnique and Microscopy. Oxford University Press, New York, NY.

Sarkanen, K.V., Ludwig, C.H., 1971. Definition and nomenclature. In: Sarkanen, K.V., Ludwig, C.H. (Eds.), Lignins – Occurrence, Formation, Structure and Reactions. Wiley Interscience, New York, NY, pp. 1–18.

Sarkanen, S., 1998. Template polymerization in lignin biosynthesis. In: Lewis, N.G., Sarkanen, S. (Eds.), Lignin and Lignan Biosynthesis, vol. 697. ACS Symposium Series, Washington, DC, pp. 194–208.

Sarni, F., Grand, C., Boudet, A.M., 1984. Purification and properties of cinnamoyl-CoA reductase and cinnamyl alcohol dehydrogenase from poplar stems (*Populus* X *euramericana*). Eur. J. Biochem. 139, 259–265.

Sewalt, V.J.H., Ni, W., Blount, J.W., Jung, H.G., Masoud, S.A., Howles, P.A., Lamb, C., Dixon, R.A., 1997. Reduced lignin content and altered lignin composition in transgenic tobacco down-regulated in expression of L-phenylalanine ammonia-lyase or cinnamate 4-hydroxylase. Plant Physiol. 115, 41–50.

Suzuki, M., Kamide, Y., Nagata, N., Seki, H., Ohyama, O., Kato, H., Masuda, K., Sato, S., Kato, T., Tabata, S., Yoshida, S., Muranaka, T., 2004. Loss of function of 3-hydroxy-3-methylglutaryl coenzyme A reductase 1 (HMG1) in *Arabidopsis* leads to dwarfing, early senescence and male sterility, and reduced sterol levels. Plant J. 37, 750–761.

Taylor, N.G., Howells, R.M., Huttly, A.K., Vickers, K., Turner, S.R., 2003. Interactions among three distinct CesA proteins essential for cellulose synthesis. Proc. Natl. Acad. Sci. USA 100, 1450–1455.

Taylor, N.G., Laurie, S., Turner, S.R., 2000. Multiple cellulose synthase catalytic subunits are required for cellulose synthesis in *Arabidopsis*. Plant Cell 12, 2529–2539.

Taylor, N.G., Scheible, W.R., Cutler, S., Somerville, C.R., Turner, S.R., 1999. The *irregular xylem3* locus of *Arabidopsis* encodes a cellulose synthase required for secondary cell wall synthesis. Plant Cell 11, 769–780.

Towers, G.H.N., Gibbs, R.D., 1953. Lignin chemistry and the taxonomy of higher plants. Nature 172, 25–26.

Turner, S.R., Somerville, C.R., 1997. Collapsed xylem phenotype of *Arabidopsis* identifies mutants deficient in cellulose deposition in the secondary cell wall. Plant Cell 9, 689–701.

Wengenmayer, H., Ebel, J., Grisebach, H., 1976. Enzymatic synthesis of lignin precursors. Purification and properties of a cinnamoyl-CoA:NADPH reductase from cell suspension cultures of soybean (*Glycine max*). Eur. J. Biochem. 65, 529–536.

Wiesner, J., 1878. Note über das Verhalten des Phloroglucins und einiger verwandter Körper zur verholzten Zellmembran. Sitzungsberichte der Kaiserlichen Akademie der Wissenschaften. Math. Nat. Classe 77, 60–66.